Thermal Properties and Phase Morphology of Melt-Mixed Poly(trimethylene terephthalate)/Poly(hexamethylene isophthalamide) Blends

Fang-Chyou Chiu, Hwung Yi Lee, Yu Hsuan Wang

Department of Chemical and Materials Engineering, Chang Gung University, Tao-Yuan 333, Taiwan, Republic of China

Received 1 May 2007; accepted 28 June 2007
DOI 10.1002/app.27556
Published online 7 December 2007 in Wiley InterScience (www.interscience.wiley.com).

ABSTRACT: This work examines the thermal properties and phase morphology of melt-mixed poly(trimethylene terephthalate) (PTT)/poly(hexamethylene isophthalamide) (PA 6I) blends. Two temperatures, i.e., 250 and 260°C, are used to prepare the blends, respectively. Differential scanning calorimetry results indicate the immiscible feature of the blends. It is thus concluded that the ester-amide interchange reaction hardly occurred in the PTT/PA 6I blends. Depending on the composition and mixing temperature, the crystallization ability of PTT in the blends is either enhanced or hindered. Basically, a lower PA 6I content shifts the PTT melt crystallization to a higher temperature, whereas a higher PA 6I content causes an opposing outcome. The original complex melting behavior of neat PTT becomes more regular after the incorporation of 60 wt % or 80 wt % of PA 6I. Thermogravimetry analyses (TGA) show that the thermal stability of the blends improves as the PA 6I content increases. The two-phased morphology of the blends is examined by scanning electron microscopy (SEM). Polarized light microscopy (PLM) results reveal that the PTT spherulites become coarser with the inclusion of PA 6I; only smaller/dispersed crystallites are observed in the blend with 20 wt % of PTT. © 2007 Wiley Periodicals, Inc. J Appl Polym Sci 107: 3831–3839, 2008

Key words: PTT; PA 6I; blend; thermal properties; phase morphology

INTRODUCTION

Polymer blends continue to attract much attention both academically and industrially due to their potential to exhibit tailor-made properties.[1,2] Of all the blend systems studied, the aromatic polyester-included blends have always been one of the main interests. One reason for this is that aromatic polyesters represent a major class of engineering plastics with excellent properties and a large variety of applications. As a consequence, the aromatic polyester-included blends are expected to possess a wide range of features that will enhance the applications of homopolyesters. Another reason is the interchange reactions that they can possibly undergo with other polyesters[3–6] or polyamides[7,8] in certain environments. Therefore, if one is capable of controlling the extent of the interchange reactions, miscible blends as well as tailored block and/or random copolymers can be formed with desirable properties.

In the past decade, a new aromatic polyester, poly (trimethylene terephthalate) (PTT), was commercialized.[9,10] Its mechanical properties are evaluated to be comparable to those of PET and PBT. Hence, it offers the promise of market opportunities for fiber, film, and engineering plastics. Other properties of PTT have also been studied.[11–16] For examples, its crystallization kinetics and melting behavior were reported by Huang and Chang[14] and Hong et al.[15] Unsurprisingly, some studies on the PTT-included blends were conducted. Poly(ether imide) and poly(ethylene-*co*-cyclohexane 1,4-dimethanol terephthalate) are the miscible counterparts reported for PTT.[17,18] The various thermal properties of the two blend systems were examined. Blends of PTT with immiscible counterparts of polystyrene and polyamide-12 (PA 12) were also investigated.[19,20] More recently, the miscibility and phase behavior of the blends of PTT with polycarbonate (PC) were studied. Particularly, Lee and Woo[21] indicated that the solution-cast PTT/PC blends were inherently immiscible, but after annealing at 260°C, the blends could become miscible because of the transesterification reaction. Meanwhile, the author and his colleague[22] showed that while being melt-mixed at 280°C, the shorter-time mixed PTT/PC blends were partially miscible, and the blends changed to a miscible state after a longer time of mixing.

Correspondence to: F.-C. Chiu (maxson@mail.cgu.edu.tw).
Contract grant sponsor: National Science Council of the Republic of China (Taiwan); contract grant number: NSC92-2216-E-182-003.

According to previous reports, it can be concluded that the possible interchange reaction plays an important role in controlling the properties of PTT-included blends. Therefore, from either of the academic or industrial viewpoint, it is essential to study the possibility of interchange reaction between the newly commercialized PTT and engineering polyamides. In this article, the results of our study on the blends of PTT with an amorphous polyamide (poly (hexamethylene isophthalamide), PA 6I) are reported. Two different temperatures of 250 and 260°C, respectively, were employed to melt-mix the two components. The blends' thermal properties and phase morphology were evaluated by differential scanning calorimetry (DSC), thermogravimetry, scanning electron microscopy (SEM), and polarized light microscopy (PLM). As a result, whether or not the interchange reaction occurred in the blended system was determined.

EXPERIMENTAL

Materials and blends preparation

PTT in pellet form was supplied by Union Chemical Laboratories (Industrial Technology Research Institute, Taiwan). The intrinsic viscosity measured in the phenol/tetrachloroethane (60/40 weight ratio) solvent at 25°C is ca. 0.95 dL/g. PA 6I (Grivory 21) with a density of 1.18 was purchased from EMS-FAR EASTERN. An Atlas Laboratory Mixing Molder was used to prepare the samples of different compositions (PTT/PA6I: 100/0, 80/20, 60/40, 40/60, 20/80, and 0/100) based on weight percentage at 250 and 260°C, respectively, for 10 min with a rotor speed of 60 rpm. Before the mixing, PTT and PA 6I were dried under vacuum at 100°C for at least 5 h to minimize the possibility of hydrolysis during the mixing processes.

Characterizations

The thermal properties (including T_g's, crystallization behavior, and melting behavior) of the neat components and the blends were investigated using a Perkin–Elmer DSC 7 analyzer equipped with an intercooler. The heat flow and temperature of DSC were calibrated with standard materials, indium, and zinc. Nitrogen gas was consistently purged during the scans. For T_g and cold crystallization measurements, the samples were first melted at 260°C for 2 min, and then quenched with liquid N_2 to obtain an amorphous characteristic. The amorphous samples were further heated at a rate of 20°C/min to the melt state. For melt crystallization experiments, the samples were cooled from the melt with 10°C/min and 40°C/min, respectively, to room temperature. The crystallized samples were subsequently heated to the melt state for the corresponding melting behavior investigations. The thermal stability of the samples was characterized using a thermogravimetric analyzer (TGA) on a TA Instruments Q-50 system under an air environment. The heating process was conducted from room temperature to 750°C at a rate of 20°C/min.

The phase morphology of fractured samples was investigated by a scanning electron microscope (SEM, JEOL JSM-5410). The samples were prepared by fracturing them in liquid nitrogen. An Olympus BH-50 polarized light microscope (PLM) in conjunction with a Linkam THMS 600 hot stage were employed for the samples' crystalline morphology observation. The thin-film specimens were prepared by melting the samples at 260°C first, and then compressing them between glass slides.

RESULTS AND DISCUSSION

Glass transition temperature and cold crystallization

It is well recognized that the miscibility of binary blend systems can be discussed in terms of the appearance of either single T_g or double T_g's. Figure 1(a) shows the DSC heating thermograms of liquid N_2 quenched 250°C-treated/mixed samples. The T_g's of the neat PTT and PA 6I are determined to be 44.6°C and 124.8°C, respectively. For each of the blends, two T_g's that are hardly different from those of the neat components are observed. On the basis of the DSC results, we can conclude that PTT and PA 6I form an immiscible blend system, which is reminiscent of the PTT/PA 12 blend system.[20] Similar T_g results are observed in the 260°C-treated/mixed samples, as depicted in Figure 1(b). This is an indication that the ester-amide interchange reaction hardly occurred upon the mixing processes. In addition to the T_g's, the cold crystallization of PTT in the neat state and in the blends is also observed in the DSC thermograms, and it is found that the cold crystallization temperature (peak temperature, T_{cc}) of PTT is influenced by the incorporation of PA 6I, though the blends show an immiscible feature. The influence, indeed, is composition dependent. That is, when PA 6I is a minor component in the 250°C-mixed or 260°C-mixed blends, PTT cold crystallizes at a slightly higher temperature as compared to that of neat PTT. On the other hand, when the PA 6I content becomes 60 or 80%, PTT cold crystallizes at a comparable or slightly lower temperature than that of neat PTT. Regarding the cold crystallization enthalpy of PTT in each sample, little difference is noted after the

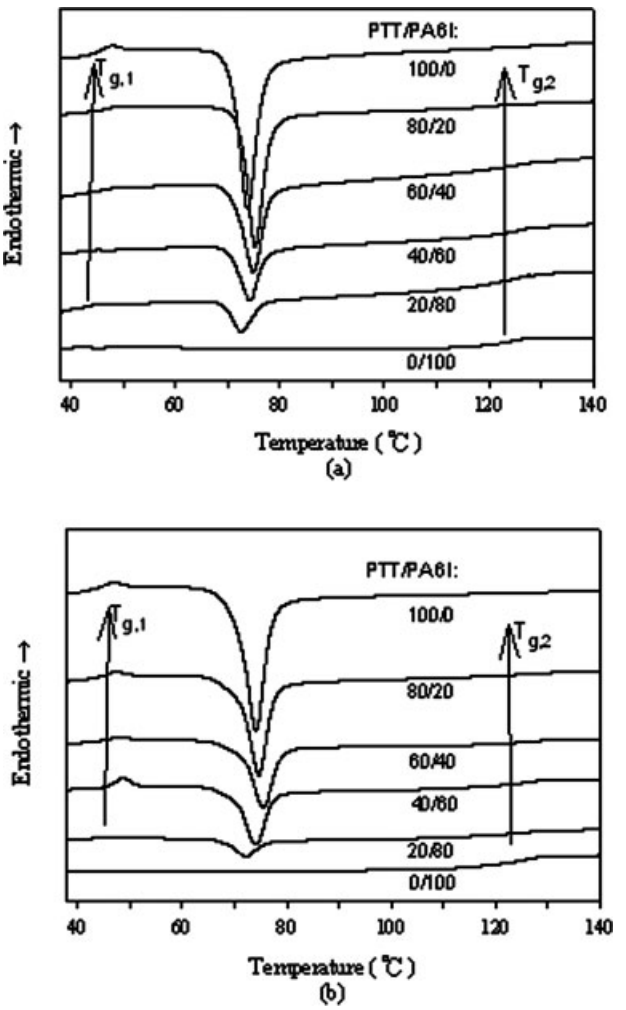

Figure 1 DSC heating thermograms of liquid nitrogen quenched samples with different mixing temperatures: (a) 250°C and (b) 260°C.

normalization based on the composition of PTT in the blends. The T_g's and T_{cc}'s of the samples determined from the DSC thermograms are listed in Table I.

Melt crystallization

Figure 2(a,b) illustrate the DSC thermograms of the 250°C-treated/mixed neat PTT and its blends cooling from the melt at the rates of 10 and 40°C/min, respectively. The incorporation of PA 6I alters evidently PTT's melt crystallization onset temperature (T_o) and peak temperature (T_{mc}), though they form immiscible blends. When the PA 6I content is 20 or 40%, the T_o and T_{mc} of PTT shift to higher temperatures, and a higher PA 6I content causes higher T_o and T_{mc}. Unexpectedly, when the PA 6I content becomes 60%, two crystallization exotherms are displayed. For example, in Figure 2(a) (under a 10°C/min cooling rate), one high-temperature exotherm shows up at around 190°C (close to that in the PTT/PA 6I-60/40 blend), and one low-temperature exotherm shows up at a much lower temperature around 96°C. When the PA 6I content further increases to become 80%, only the low-temperature crystallization exotherm exists. This interesting composition-dependent crystallization behavior is not often observed in polymer blend systems. It should be mainly attributed to the different phase morphology developed in the blends. According to the SEM results (see the following Morphology section), it is confirmed that PTT plays the matrix phase in the blends when it is the major component. On the contrary, PTT becomes the dispersed phase when it is the minor component. The shifts in PTT's crystallization to higher temperatures in the PTT/PA 6I-80/20 and -60/40 blends suggest that the dispersed PA 6I phase could serve as a nucleation agent for the PTT matrix. The higher the PA 6I content is, the higher nucleation efficiency is demonstrated. However, in the PTT/PA 6I-40/60 blend, the PTT phase inverts to become the dispersed phase with various-sized domains. The observed high-temperature exotherm can be ascribed to the occurrence of crystallization within the larger-dispersed domains (mainly through the heterogeneous nucleation mechanism, which is

TABLE I
Representative Thermal Data of the Samples Measured from DSC Scans

PTT/PA 6I	100/0	80/20	60/40	40/60	20/80	0/100
T_g (250°C)	44.6	45.2/125.3	44.5/125.1	44.2/125.8	43.2/124.4	124.8
T_g (260°C)	44.5	44.8/125.6	45.4/125.3	45.8/125.9	43.6/125.5	125.4
T_{cc} (250°C)	73.7	75.4	75.0	74.4	72.7	NA
T_{cc} (260°C)	74.0	74.7	75.4	74.3	72.0	NA
T_{mc}(250°C)[a]	176.1	183.5	190.2	190.0/96.3	87.4	NA
T_{mc}(250°C)[b]	151.2	161.9	171.9	171.2/74.5	67.9	NA
T_{mc}(260°C)[a]	173.8	174.8	176.9	96.7	85.5	NA
T_{mc}(260°C)[b]	152.5	151.2	153.8	73.2	67.9	NA

All units of the thermal data: °C.
The temperature inside the parenthesis: mixing temperature.
NA: not available.
[a] 10°C/min cooling rate.
[b] 40°C/min cooling rate.

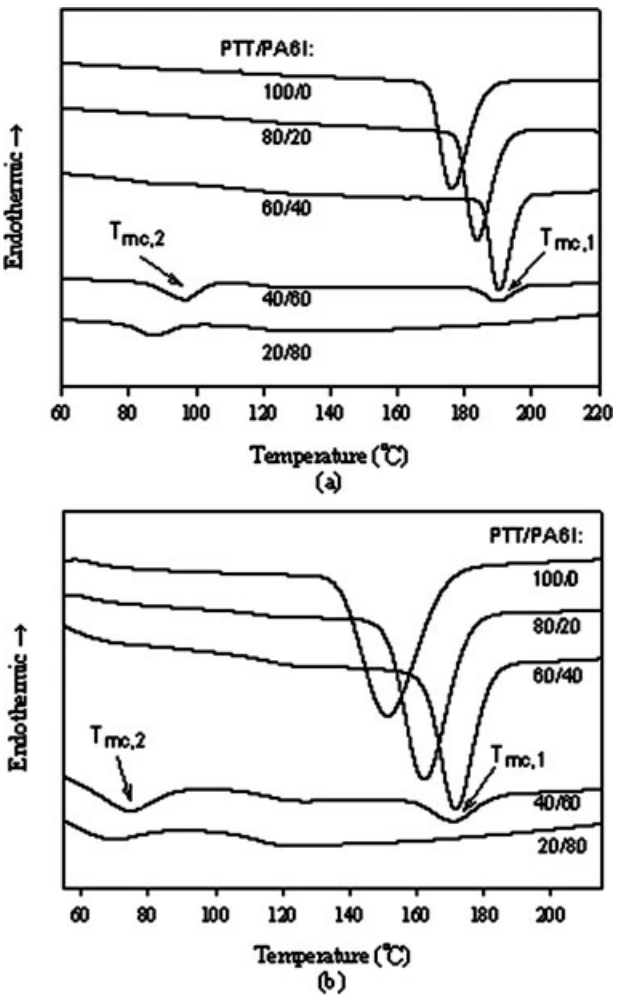

Figure 2 DSC cooling thermograms of the 250°C-treated/mixed neat PTT and its blends under different cooling rates: (a) 10°C/min and (b) 40°C/min.

similar to that in the PTT matrix of the 60/40 blend). As for the low-temperature exotherm, it should be associated with the PTT crystallization within the smaller-dispersed domains (mainly through the homogeneous nucleation mechanism[23]). As the PTT content further decreases to 20%, the larger PPT-dispersed domains as those in the 40/60 blend hardly exist. Therefore, only the homogeneously nucleated low-temperature PTT crystallization appears. The T_o and T_{mc} are even lower than those in the PTT/PA 6I-40/60 blend. Similar crystallization behaviors are also observed when the cooling rate is 40°C/min as shown in Figure 2(b).

The melt crystallization thermograms of the 260°C-treated/mixed samples are depicted in Figure 3(a,b). As compared to Figure 2, the effect of changing the mixing temperature on PTT's melt crystallization in the blends is noted, especially in the PTT-dominant blends. That is, the incorporation of 20 or 40% of PA 6I in the 260°C-mixed blend only enhances slightly (at a 10°C/min cooling rate) or even retards (at a 40°C/min cooling rate) the crystallization of PTT. PA 6I no longer facilitates the nucleation of the PTT matrix upon crystallization. The reason for the interesting observation could be attributed to the fact that a higher mixing temperature would result in a lower viscosity for each of the two components upon mixing. Accordingly, a higher extent of molecular contact (interaction) between PTT and PA 6I is induced in the melt state as well as in the solidified state. In turn, a higher extent of interaction causes a decrease in the mobility of PTT upon crystallization, since PA 6I possesses a much higher T_g as revealed in previous section. The two components might have developed a slightly partial miscible feature. To justify these speculations, the melt crystallization of PTT in higher-temperature (270°C)-mixed blends is further investigated. PA 6I is noted to hamper PTT's crystallization to a higher degree (not shown here). Furthermore, the two crystallization exotherms exhibited in the 250°C-mixed PTT/PA 6I-40/60 blend

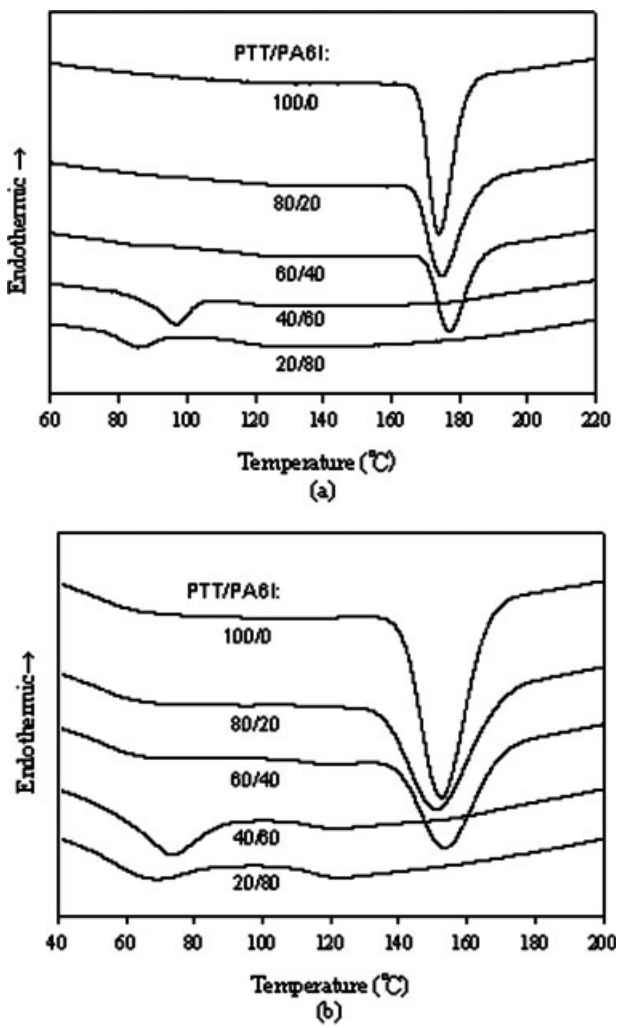

Figure 3 DSC cooling thermograms of the 260°C-treated/mixed neat PTT and its blends under different cooling rates: (a) 10°C/min and (b) 40°C/min.

becomes one low-temperature crystallization exotherm in the 260°C-mixed corresponding blend. This change indicates the more homogeneously dispersed PTT phase development in the higher-temperature mixed blend. The representative thermal data obtained from the DSC cooling scans are also included in Table I.

Melting behavior

Figure 4(a,b) illustrate the DSC melting curves of the 250°C-treated/mixed neat PTT and its blends. As anticipated, the complex melting behavior (melting–recrystallization–remelting[14,18]) of neat PTT is observed, irrespective of the precooling rate. Furthermore, the blends with 20 and 40% of PA 6I incorporations exhibit a similar complex melting behavior. Nevertheless, the recrystallization (shallow exotherm) of PTT shifts to higher temperatures in the blends, and it increases with the PA 6I content.

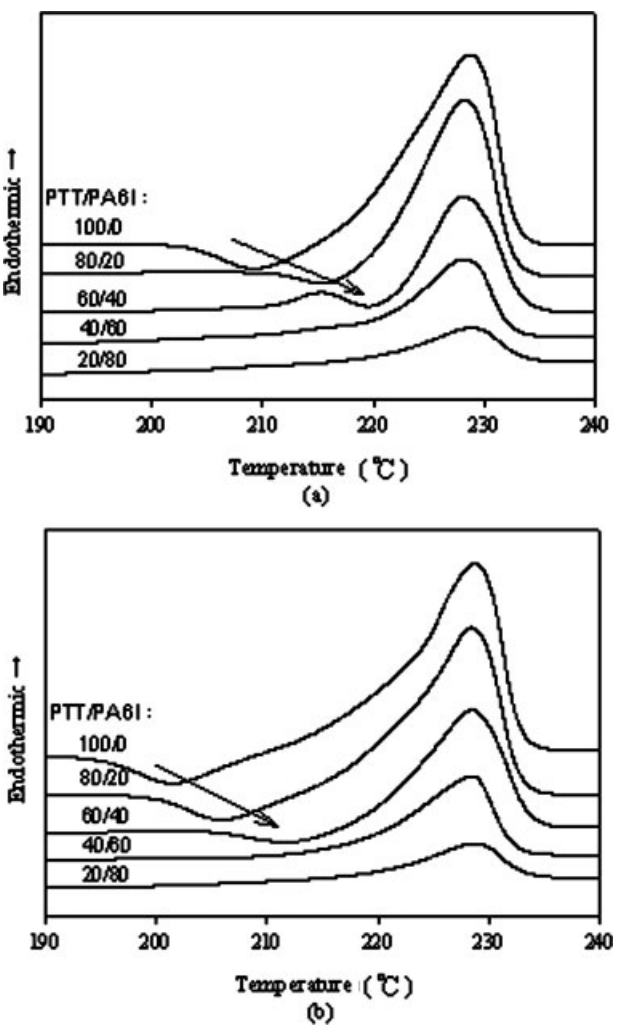

Figure 4 DSC melting thermograms of the 250°C-treated/mixed neat PTT and its blends after melt crystallization at different cooling rates: (a) 10°C/min and (b) 40°C/min.

These interesting melting behaviors have never been reported to our knowledge. The following fact might be taken into account for the observation. As revealed in the melt crystallization results [Fig. 2(a,b)], the additions of PA 6I (20 and 40%) shift the PTT crystallization to higher temperatures. The higher-temperature-crystallized PTT crystals might be more stable than lower-temperature-crystallized crystals. Accordingly, upon subsequent heating processes, more stable crystals will melt at higher temperatures and then recrystallize at higher temperatures. More interestingly, the complex melting behavior of PTT is absent in the PTT/PA 6I-40/60 and -20/80 blends, regardless of the precooling rate. That is, only a simple/regular PTT melting peak is exhibited for each of the two blends. As recalled from the melt crystallization results again, homogeneously nucleated PTT crystallization predominates in these two blends. The homogeneously nucleated crystals might be stable enough; as a result, the melting-recrystallization stages to develop more stable crystals are thus prevented upon the subsequent heating processes. Another point noticed in the figures is that the melting temperature of PTT hardly changes in the 250°C-treated/mixed samples.

The DSC melting traces of the 260°C-treated/mixed samples are illustrated in Figure 5(a,b). The complex melting behavior shows up again in neat PTT as well as in the blends with 20 and 40% of PA 6I incorporations. Nevertheless, while compared with those of the 250°C-mixed corresponding blends, the PTT recrystallization exotherm shifts only slightly to higher temperatures (10°C/min cooled samples) or is even retained (40°C/min cooled samples) in the 260°C-mixed blends. As illustrated in Figure 3(a,b), the addition of 20 or 40% of PA 6I increases slightly or even unchanges the melt crystallization temperature of PTT. Therefore, it is speculated that the stability of the PTT crystals developed is little different from one another in the neat state or in the two blends. The melting-recrystallization behavior hence resembles one another. These observations can further support the explanation we provided for the recrystallization exotherm alteration in the 250°C-mixed blends. When PTT becomes a minor component (40 and 20%) in the blends, a simple/regular melting peak (similar to that of corresponding 250°C-mixed samples) is again observed. Furthermore, the PTT melting temperature of the 260°C-treated/mixed samples declines slightly with the increase in PA 6I content. This phenomenon further suggests that the interaction (molecular contact) between PTT and PA 6I is enhanced as the mixing temperature increases. A limited miscibility of the two components may be confirmed, and the degree of perfection for the PTT crystals developed may also decrease with the presence of PA 6I. While com-

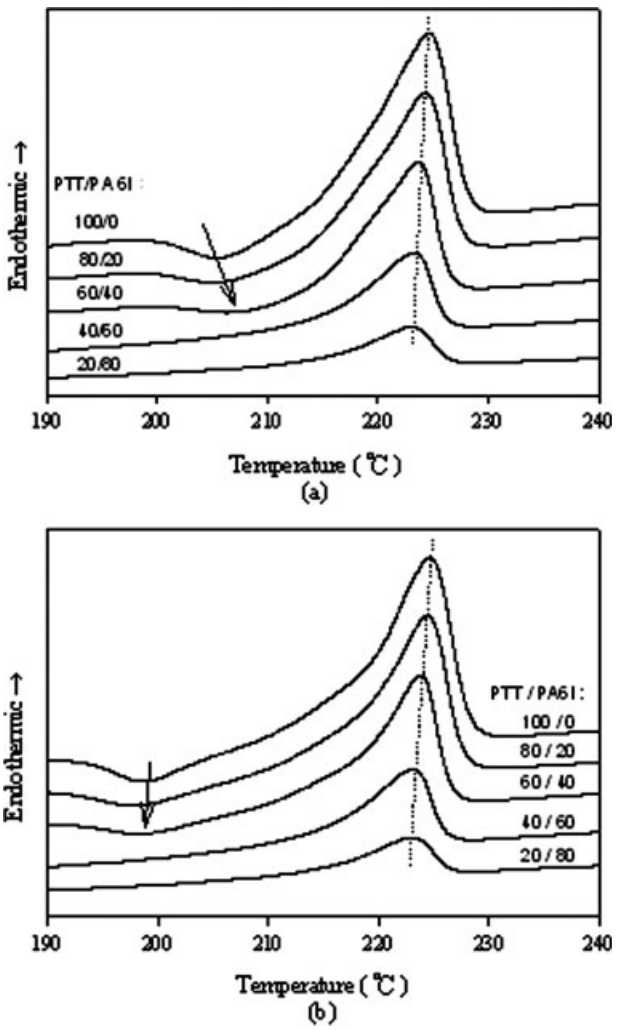

Figure 5 DSC melting thermograms of the 260°C-treated/mixed neat PTT and its blends after melt crystallization at different cooling rates: (a) 10°C/min and (b) 40°C/min.

paring the melting behaviors of the 250°C-treated/mixed samples with those of the 260°C-treated/mixed samples in more detail, it is noted that the 260°C-treated/mixed sample shows a lower melting temperature than its corresponding 250°C-treated/mixed sample. These results can be ascribed to the slight decline in PTT's molecular weight (intrinsic viscosity decreases) as it is thermally treated through a higher temperature of 260°C.

Thermal stability

The thermal stability of the prepared samples was evaluated by TGA. Figure 6(a) shows TGA scans of the 250°C-treated/mixed neat components and their blends. The neat PA 6I is noted to exhibit the highest degradation temperature among the samples, whereas the neat PTT shows the lowest degradation temperature. A multistage degradation curve is observed for each of the blends, and the curve shifts to a higher temperature with a higher PA 6I content. A similar trend in the thermal stability is also observed for the 260°C-treated/mixed samples [Fig. 6(b)]. By comparing Figure 6(a) with 6(b), it is determined that the samples of the same composition exhibit similar degradation curves. This result indicates that increasing the mixing temperature from 250 to 260°C affects less the thermal stability of the samples, further suggesting that the possible ester-amide interchange reaction hardly occurred.[22] Some representative degradation data obtained from Figure 6(a,b) are listed in Table II.

Morphology

The SEM micrographs of the 250°C-mixed blends are illustrated in Figure 7(a–d). Two apparent phases are observed in each of the blends, confirming the immiscible feature of the PTT/PA 6I blend system. To ascertain the location of the PA 6I component, formic acid was employed to etch out the PA 6I phase in the blends. Figure 8(a–c) depict the typical formic

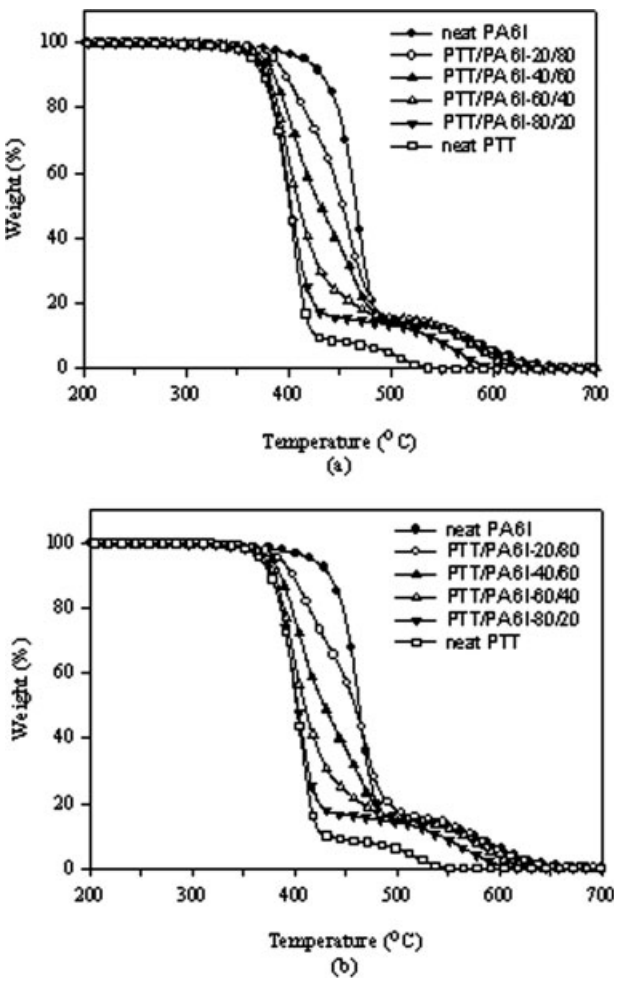

Figure 6 TGA scans of: (a) the 250°C-treated/mixed samples and (b) the 260°C-treated/mixed samples.

TABLE II
Representative TGA Data of Different Temperature-Treated/Mixed Samples

PTT/PA 6I	$T_{d(5\%)}$ (°C)	$T_{d(20\%)}$ (°C)	$T_{d(40\%)}$ (°C)
100/0 (250°C)	364.2	384.7	396.4
100/0 (260°C)	366.7	386.1	397.4
80/20 (250°C)	367.6	386.3	397.7
80/20 (260°C)	367.7	386.6	398.1
60/40 (250°C)	371.5	389.4	402.7
60/40 (260°C)	370.9	389.2	402.0
40/60 (250°C)	376.0	396.9	417.4
40/60 (260°C)	376.8	397.1	415.6
20/80 (250°C)	386.4	414.2	443.9
20/80 (260°C)	385.8	413.9	446.7
100/0 (250°C)	414.9	447.4	461.3
100/0 (260°C)	416.8	446.8	459.2

$T_{d(\alpha\%)}$, decomposition temperature at α% weight loss; the temperature inside the parenthesis: mixing temperature.

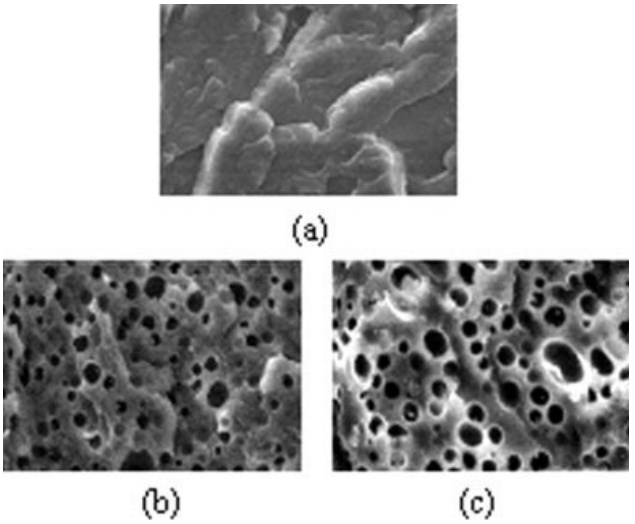

Figure 8 Representative SEM micrographs of formic acid-treated samples: (a) neat PTT, (b) PTT/PA 6I-80/20 and (c) PTT/PA 6I-60/40.

acid-treated samples. The PTT-dominant (matrix) phase morphology with various sizes of holes representing the PA 6I phase is observed in the blends. Accordingly, Figure 7(a–d) reveal the evolution from a PTT-dominant (i.e., PA 6I is the dispersed phase) phase morphology to a PA 6I-dominant (i.e., PTT becomes the dispersed phase) phase morphology with an increase in the PA 6I content. The average size of the dispersed domain increases with its concentration in the blends. Further worth noting is the fact that the dispersed PTT phase in PTT/PA 6I-40/60 blend forms two kinds of textures including larger rod-like domains as well as smaller sphere-like domains. The different-sized PTT domains are taken into account for the occurrences of two crystallization exotherms during the cooling processes as discussed in previous DSC melt crystallization results. Figure 9(a–d) show the micrographs of 260°C-mixed blends. A similar development of phase morphology with composition to that of the 250°C-mixed blends is observed, except that the rod-like PTT dispersed domains no longer exists in the PTT/PA 6I-40/60 blend. Only sphere-like PTT domains are present. Moreover, the boundary between the matrix and the dispersed phase seems to be more diffused as compared to that in the 250°C-mixed blends, suggesting slight interaction enhancement

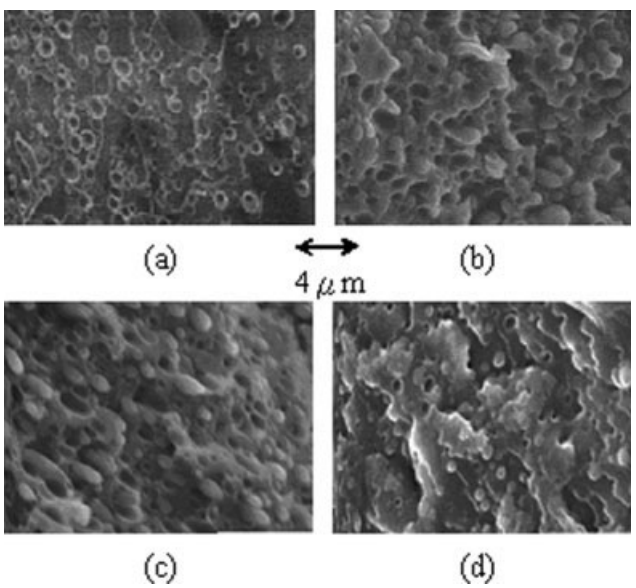

Figure 7 SEM micrographs of the 250°C-mixed blends: (a) PTT/PA 6I-80/20, (b) PTT/PA 6I-60/40, (c) PTT/PA 6I-40/60, and (d) PTT/PA 6I-20/80.

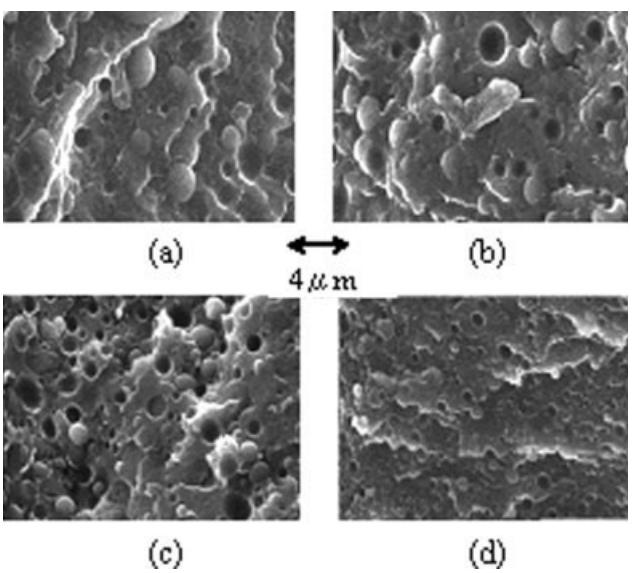

Figure 9 SEM micrographs of the 260°C-mixed blends: (a) PTT/PA 6I-80/20, (b) PTT/PA 6I-60/40, (c) PTT/PA 6I-40/60, and (d) PTT/PA 6I-20/80.

between PTT and PA 6I components with increasing mixing temperature.

The PTT crystalline morphology of the 10°C/min melt crystallized samples is observed through PLM. Figure 10(a–e) show the micrographs of 250°C-treated/mixed samples. PTT spherulites are grown in neat PTT as well as in PTT-dominant blends. However, the spherulites' size decreases after adding a certain amount of the PA 6I component [Fig. 10(b,c)], implying the accelerated PTT nucleation by PA 6I. This observation is in agreement with the DSC melt crystallization results. That is the PTT crystallization onset temperatures observed in the DSC curves shift evidently to higher temperatures after the additions of 20 and 40% of PA 6I. Further observed in these figures is that the PTT spherulites become less perfect with an increasing PA 6I content. This is because of the inclusion of the PA 6I component within the spherulites. For the PA 6I-dominant blends [Fig. 10(d,e)], no large spherulites are observed. Only small PTT spherulites and/or crystallites display. For the 260°C-treated/mixed samples, as shown in Figure 11(a–e), a similar trend in the PTT crystalline morphology evolution is observed. Nevertheless, the spherulites' size declines not so evidently as those of the corresponding 250°C-mixed PTT/PA 6I-80/20 and -60/40 blends. This means the PA 6I plays little nucleation agent role in the 260°C-mixed blends, which is consistent with the DSC crystallization data.

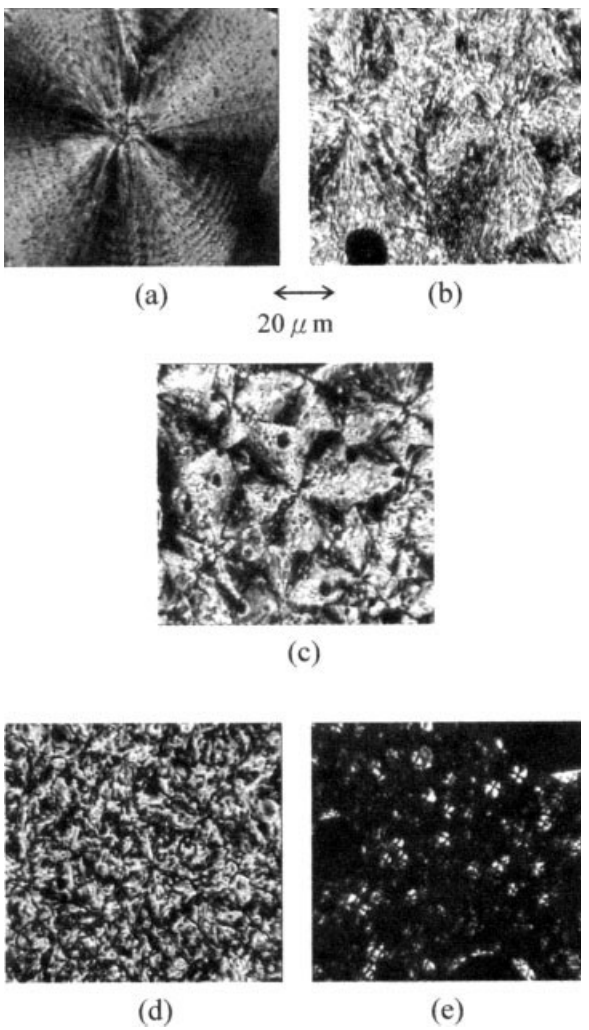

Figure 10 PLM micrographs of the 250°C-treated/mixed samples: (a) neat PTT, (b) PTT/PA 6I-80/20, (c) PTT/PA 6I-60/40, (d) PTT/PA 6I-40/60, and (e) PTT/PA 6I-20/80.

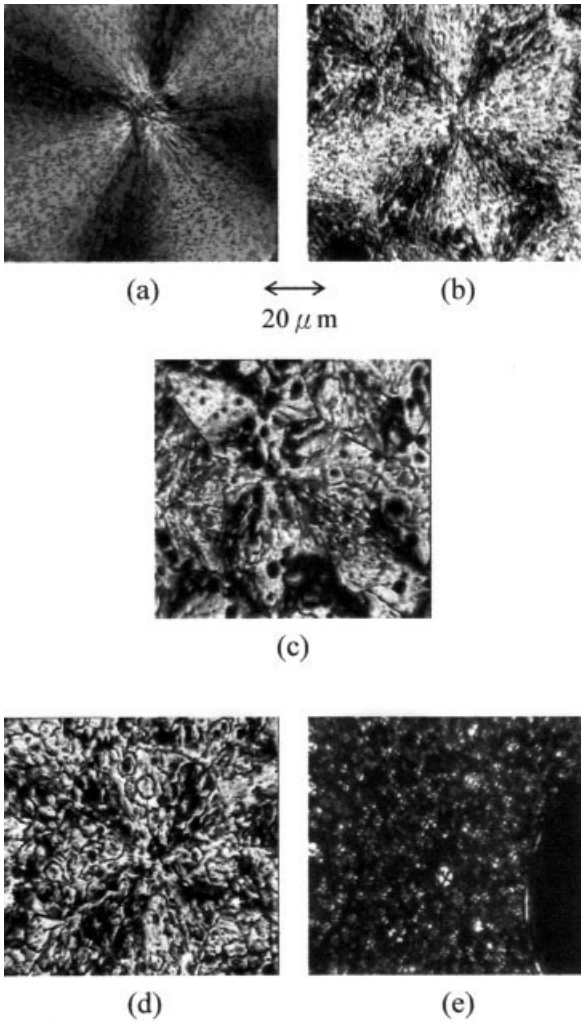

Figure 11 PLM micrographs of the 260°C-treated/mixed samples: (a) neat PTT, (b) PTT/PA 6I-80/20, (c) PTT/PA 6I-60/40, (d) PTT/PA 6I-40/60, and (e) PTT/PA 6I-20/80.

CONCLUSIONS

Two different temperatures were employed to prepare the PTT/PA 6I blends of different compositions. The T_g's of the blends suggested that the blends were immiscible regardless of the mixing temperature. The crystallization of the PTT was either facilitated or hindered in the blends, depending

on the composition and mixing temperature. PA 6I could serve as a nucleation agent for PTT in the PTT-dominant blends. Nevertheless, the nucleation efficiency declined as the mixing temperature was increased from 250 to 260°C. The unusual homogeneously nucleated PTT crystallization, causing a much lower PTT melt crystallization temperature, was observed in the PA 6I-dominant blends. The complex melting behavior of PTT with different recrystallization temperatures was observed for the 250°C-prepared neat PTT and the PTT-dominant blends. As the mixing temperature was increased, the complex melting behavior of the neat PTT and the blends resembles one another. Only simple/regular PTT melting behavior showed up for the PA 6I-dominant blends. The thermal stability of the samples was hardly affected by an increase in the mixing temperature, and a higher PA 6I content in the samples led to a higher thermal stability. Moreover, the morphology studies revealed a similar evolution of two-phased morphology with composition for the different-temperature mixed samples. The 250°C-mixed PTT/PA 6I-40/60 blend particularly exhibited two types of PTT dispersed domains which resulted in two distinct crystallization exotherms upon its cooling from the melt. The PTT spherulites were grown in neat PTT as well as in the blends. Basically, the spherulites' size decreased, and their texture became coarser as the PA 6I content was increased. On the basis of the results of thermal properties and morphology, it was therefore concluded that the possible ester-amide interchange reaction hardly occurred in the PTT/PA 6I blends investigated.

References

1. Utracki, L. A. Commercial Polymer Blends; Chapman & Hall: New York, 1998.
2. Folkes, M.; Hope, P., Eds. Polymer Blends and Alloys; Blackie Academic & Professional: London, 1993.
3. Porter, R. S.; Wang L. H. Polymer 1992, 33, 2019.
4. Yang, H.; He, J.; Liang, B. J Polym Sci Polym Phys Ed 2001, 39, 2607.
5. Kenwright, A. M.; Peace, S. K.; Richards, R. W.; Bunn, A.; MacDonald, W. A. Polymer 1999, 40, 5851.
6. Liu, S.; Li, W.; Liang B.; Yu, Y. Eur Polym Mater 2000, 36, 2159.
7. Ho, J. C.; Wei, K. H. J Polym Sci Polym Phys Ed 2000, 38, 2124.
8. Kim, B. K.; Baek, S. H.; Kim, M. S. J Appl Polym Sci 2004, 91, 3966.
9. Chuah, H. H. Chem Fiber Int Sci 1996, 46, 424.
10. Dangayach, K.; Chuah, H. H.; Gergen, W.; Dalton, P.; Smith, F. 55th ANTEC Proceedings 1997, p 2097.
11. Wang, B.; Li, C. Y.; Hanzlicek, J.; Cheng, S. Z. D.; Geil, P. H.; Grebowicz, J.; Ho, R. M. Polymer 2001, 42, 7171.
12. Pyda, M.; Boller, A.; Grebowicz, J.; Chuah, H.; Lebedev, B. V.; Wunderlich, B. J Polym Sci Polym Phys Ed 1998, 36, 2499.
13. Pyda, M.; Wunderlich, B. J Polym Sci Polym Phys Ed 2000, 38, 622.
14. Huang, J. M.; Chang, F. C. J Polym Sci Polym Phys Ed 2000, 38, 934.
15. Hong, P. D.; Chung W. T.; Hsu, C. F. Polymer 2002, 43, 3335.
16. Chen, X.; Hou, G.; Chen, Y.; Yang, K.; Dong, Y.; Zhou, H. Polym Test 2007, 26, 144.
17. Kuo, Y. H.; Woo, E. M.; Kuo, T. Y. Polym J 2001, 33, 920.
18. Chiu, F. C.; Huang K. H.; Yang, J. C. J Polym Sci Polym Phys Ed 2003, 41, 2264.
19. Huang, J. M. J Appl Polym Sci 2003, 88, 2247.
20. Asadinezhad, A.; Yavari, A.; Jafari, S. H.; Khonakdar, H. A.; Bohme, F.; Hassler, R. Polym Bull 2005, 54, 205.
21. Lee, L. T.; Woo, E. M. Colloid Polym Sci 2004, 282, 1308.
22. Chiu, F. C.; Ting, M. H. Polym Test 2007, 26, 338.
23. Wunderlich B. Macromolecular Physics; Academic Press: New York, 1976; Vol. 2.